A Study on the Engineering Considerations for the Unglazed Transpired Solar Air Heaters (Utsah) Design Under the Egyptian Conditions

Hassanain, A. A.
Agriculture Engineering Department; Faculty Of Agriculture Suez Canal University Ismailia- Egypt
(Received, December 6, 2004)

ABSTRACT

Investigates were conducted inside a controlled solar simulator room (of 3.2m length, 2.4m width and 3m height) to test the affecting parameters on the unglazed transpired solar air heaters design. The considered parameters were, the hole (perforation) diameters, dimensions apart, suitable suction velocity under the simulated incident solar radiation of the investigation site, effect of the prevailing wind speed and wind direction, also effect of material being used and its thickness. Heat exchange effectiveness was taken to govern and select the best design option.

Three main components were used in these investigations: the plenum wooden prism which holds the perforated plates under investigation, solar simulator and the wind tunnel which simulates the prevailing wind direction and its speed.

A prism shape wooden box of 1.5m length and 0.40m x 0.40m square cross section was used as a plenum, where the perforated plates under investigation were held by the plenum aperture which faced the solar simulator; on the other-side, a suction blower was located. Isothermal perforated plates of different materials and different thickness were investigated. Range of different isothermal good conductor metals i.e. Steel, Galvanized steel and Aluminum each has thickness of 0.5mm, 0.9mm, 1.2mm and 1.4mm, were investigated. Holes of 2mm, 3mm, 4mm, 5mm, and 6mm diameters and with different distances apart were distributed on the plates at different square shapes of 80x80mm, 40x40mm, 20x20mm and 10x10mm also different diamond shapes of 57x57mm, 29x29mm and 14x14mm. The perforated plates were investigated with different suction air flows of 1.3ms^{-1}, 0.91ms^{-1}, 0.67ms^{-1} and 0.58ms^{-1} through thin isothermal perforated plates with and without a cross wind on the upstream face.

Tungsten-halogen lamps of 2, 4, 6, and 8kW were investigated to find out the suitable illumination power resource among these resources to simulate the solar energy intensity over Ismailia region. A small wind tunnel was used to simulate the prevailing wind speed. Wind speeds of 1.51ms^{-1}, 1.35ms^{-1}, 1.29ms^{-1} and 0.86ms^{-1} were performed to find out the prevailing wind speed effect with blowing angels of 0°, 15°, 30°, 45° and 60° all were compared with no wind conditions.

Results indicated that, the heat exchange effectiveness was found increasing with the wind speed increase for the same wind-blowing angle. Apart of the wind speed of 1.51ms^{-1}, no trend was noticed for the effect of the blowing wind angle with the surface. A directly relationship was found between the heat exchange effectiveness and the wind speed in ms^{-1} for the same blowing angle. The amount of the measured radiation has a directly proportional with the simulator lamp power depending on the number of lamps in use. Meanwhile, an inverse relationship was found between the amount of radiation and the distance between the resource and the object being investigated. Using the 8kW halogen solar simulator can simulate the amount of the solar radiation flux on Ismailia region (Latitude of 30.58°N and Longitude of 32.23 °E), which varies between 424Wm^{-2} to 659Wm^{-2} where the study was conducted to find out the best design options for the unglazed transpired solar air heaters.

INTRODUCTION

The transpired solar collector concept plays an important role in solar thermal applications. For instance it can be used in crop drying and building ventilation as a way to reduce the energy requirements of these processes. The required fans for these processes can be powered by photovoltaic cells to reduce the operating cost. **(Gawlik, 1998)**.

Unglazed transpired-plate solar air-heaters are effective devices where outside air is to be heated directly for heating/ventilation purposes. As the outside air in question is drawn straight from ambient, uniformly through the whole surface of a perforated blackened plate (the absorber plate). The glazing traditionally used for reducing radiant and convective head losses from the plate of the covered solar collectors can be dispensed within this situation. The convective boundary layer is continually sucked off, thus virtually eliminating the convective loss, and the intimate heat transfer between the plate and the sucked air keeps the plate temperature low, minimizing the radiant loss **(Cao et al., 1993)**.

The heat exchange effectiveness measure the effectiveness of the air to sweep and gain surface temperature, it is taken as indicator for how much, the temperature gained from the surface. It is a ratio of the air temperature

increase above ambient to the surface temperature increase above ambient. For solar collector applications, high effectiveness values are mostly of interest, given as **Kutscher and Christensen (1992)** Also, **Dymond and Kutscher (1995)** as:

$$h\varepsilon_x = \frac{T_o - T_a}{T_s - T_a} \qquad (1)$$

The hole-diameter, which matches with the suction velocity and the effect of the material of the unglazed systems, needs more research (**Hassanain , 2003**). To carry out such research, it should be repeatable investigations so it cannot be achieved in the open conditions under the direct sunrays. It is carried out inside controllable lab under solar simulator techniques.

Simulation of the solar radiation depends up-on the kind of the investigation that will be carried out under that simulator. For instance, the spectrum in the range of the solar heat rays region must be simulated for the solar thermal experiments. Within such of these experiments, the performance of the collectors being tested is affected by the thermal radiation of the indoor environment in which it operates, walls and air temperatures are approximately equal **(Green and Gillett, 1979)**. Visible light also required for the phtovoltaic experimentation, as the light-source luminous density must be considered for the investigations of solar energy conversion into electrical energy **(Pekruhn and Germer, 1980)**. Both of the visible and heat rays are required to carry out the thermal and photovoltaic investigations.

The most commonly used light sources for the purposes of simulating the artificial sunlight are the xenon lamps, the compact iodide daylight (CID), tungsten-halogen lamps (THL). The xenon lamps are producing by far the best spectral matching to daylight but are seldom used, as they are very expensive and require extensive cooling arrangements. CID lamps are widely used in simulators, but are only good for simulating sunlight conditions for thermal uses. This is due to the spectral distribution of light from these lamps, which is sensitive for photovoltaic conversion (**Ahmed, 1991**). Seven compact Iodide Daylight (CID) lamps were mounted at the UK in 1995. The lamps were selected to simulate the solar thermal their output spectrum, which resembles direct normal irradiance at air mass (AM) of 1.5. (**Ulster University Newsletter, 1995**). The air mass is the ratio of the mass of atmosphere through which beam radiation passes to the mass it would pass through if the sun were at the zenith, i.e. directly overhead, (**Duffy and Beckman, 1991**). Better spectral matching for sunlight simulation is achieved by the use of Tungsten-Halogen Lamps (THL), although these lack output in the ultraviolet portion of the spectrum and have a larger proportion of infrared light (**Ahmed, 1991**).

Kamanga, (1987) used tungsten halogen lamps, which cover a spectral range of 200-2500 x 10^{-9}meters within his experiments campaign in the UK as, the planck distribution of these lamps was compared with that of the sun at 6000K to ascertain the region where the spectral emissive power concentrated. The graph that was given for the distribution showed that most of the radiation flux from the lamps falls within the required short wavelength for the solar collection of 0.25 to 2.5 x 10^{-6}meter.

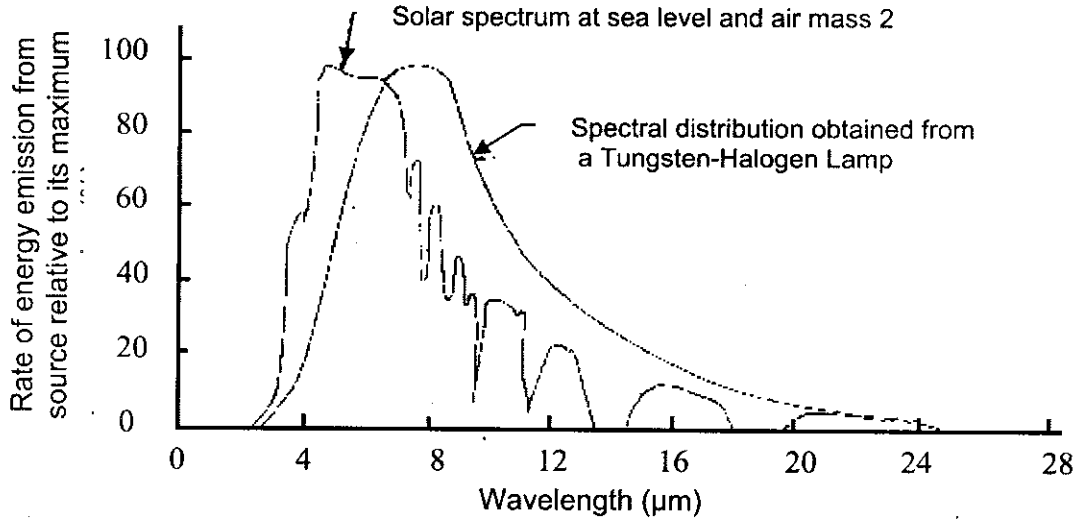

Figure (1): Comparison between the spectral distribution of light from the Halogen lamps and the solar spectrum under AM2 illumination (**Ahmed, 1991**).

Comparing the characterization of the sunlight within the visible light and the infrared region and with that of the halogen light. It was found that, it could be used to simulate the sunrays for the experiments in repeatable conditions for the thermal and photovoltaic applications. Also, comparing the spectral distribution of radiation from these lamps and that of the solar spectrum under the air mass of the site showed a fairly good match over most parts of the spectrum, as it is shown in figure (1).

The objective of this study is to investigate some of the engineering parameters, which will be required for the unglazed transpired solar air heaters (UTSAH) design under the Egyptian conditions. Heat exchange effectiveness was considered to be the comparable factor within this study to find out the suitable parameter that matches the climatic condition of the investigation site. These investigated parameters are the suitable suction airflow rate, hole diameters and spacing between holes for different investigated materials with different thickness, the effect of the wind speeds and wind directions were all considered.

MATERIALS AND METHODS

The experimental rig, which was used in this study, is given in figure (2). It consisted of three main components; the plenum wooden box with the plates under investigations, solar simulator and wind tunnel, these components are explained as follows:

Plenum:

Wood with 2.5cm thick was used to form a plenum with dimensions of 1.5m length, 0.4m width and 0.4m height. The upper side of the plenum was consisted of four gates. It was completely sealed and closed from any cracks and completely insulated. The four gates were used to add or remove the used instrumentation. Air was sucked with different suction velocities of 0.58, 0.67, 0.69, 0.91 and 1.3ms^{-1} by a Toshiba fan. An electric switch was used to vary the fan velocity as a result of the input current to obtain different suction flow rates of air. To vary the fan suction velocity, the plenum aperture was divided into small squares (1296 square, each has area of 1cm^2) and velocity of air was measured and averaged.

Different metals plates, good thermal conductors, were examined. Thickness of 0.5mm, 0.9mm, 1.2mm and 1.4mm, for each of the three metals Steel, Galvanized steel and Aluminum plates were investigated. Holes with the investigated diameters were punctured without leaving stains as a results of the perforation process were applied on the investigated plates of the different materials and different thickness. Holes of 2mm, 3mm, 4mm, 5mm, and 6mm diameters were investigated for all the investigated plates metals and thickness. The punctured holes were distributed in squares and diamonds shapes of 80x80mm, 40x40mm, 20x20mm and 10x10mm square shapes and 57x57mm, 29x29mm and 14x14mm diamond shapes. A matt black paint of 0.95 absorpitivity and emissivity (Norton, 1992) was applied on the front surface that faced the solar simulator lamps, to increase the absorbed radiation by the surface. The investigated plates were fitted precisely on the front aperture of the plenum to face the simulator lamps. Table (1) gives the thermal conductivity (k), density (ρ) and the specific heats (c_p) which were used to determine the thermal diffusivity (θ) according to equation (2) of Incropera and Dewitt (1996). For the three investigated materials steel, galvanized steel and aluminum, the thermal diffusivities (θ) was found 2.28x10^{-5}, 1.2x10^{-5} and 9.71x10^{-5} m^{2}s^{-1}, respectively

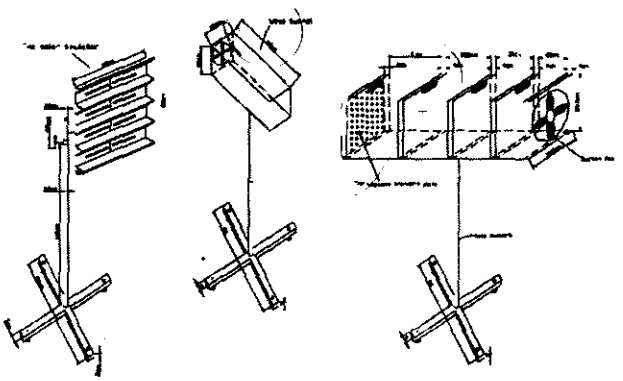

Figure (2): Investigation rig.

Table (1): Thermal conductivity, density (ρ) and specific heats (c_p) for the three investigated metals which were used as a material for the unglazed transpired solar air heaters **(Incropera and Dewitt, 1996)**.

Plate metal	Thermal conductivity (k), $W(mK)^{-1}$	Density (ρ), kgm^{-3}	Specific heat (c_p), $J(kgK)^{-1}$
Steel	80.2	7870	447
Galvanized steel	45.3	7833	480
Aluminum	237	2702	903

$$\theta = \frac{k}{\rho c_p} \qquad (2)$$

Solar simulator:

A laboratory solar simulator was constructed, it has advantages such as: getting a stable incident radiation flux to test different solar techniques either the thermal or the photovoltaic systems. Controlling the ambient air temperature and the environmental conditions where the indoor experiments are carried out.

An Aluminum-metal with a glass partition was made in a room, which has dimensions of 7.25m, 2.40m and 3.00m for the length, width and height respectively. The partition created a small room with dimensions of 3.20m, 2.40m and 3.00m for the length, width and height. The skeleton of the aluminum-metal partition was made of aluminum alloys, while the rest of the partition wall was 6mm glass thick, it was used as a hatch to follow up the experiments. A black curtain was used to cover the two ventilation vents (which had dimensions of 0.85m x0.35m each) for darkening the room as it is shown in figure (A1) in the appendices.

Tungsten-Halogen lamps (220-240Volt, 1000Watt each), were selected to simulate the solar radiation. The lamps were manufactured by phoenix Electric Co., Ltd. Japan, it has a diameter of 7.4mm and 19cm length as it is shown in a plate in the figure (A2) in the appendices. Every two lamps were grouped in 2kW by providing on/off Seimins electric switch and automatic Siemens plug to avoid the sudden fluctuation in the building grid. Lamps were fixed in 0.4mm thick reflective aluminum trove channel shape with 0.08m ... small side and 0.14m for the aperture side. An aluminum enclosure with 0.6m length and 0.58m width was constructed to fix the four trove rows.

A vertical telescopic cylindrical stand was assembled to carry the lamp tray, it enables the simulator lamp tray to rotate 360° horizontally and vertically as shown in figure (A3) in the appendixes.

Simulator ray tracing:

The emitted rays from the solar simulator were traced theoretically using the basic light laws for the illuminated flux from the cylindrical shape lamp which is shown in figure (A2) in the appendices. The ray tracing was considered for the four simulator troves, each has 2 lamps in a cylindrical shape with 360° for a 7.4mm diameter and length of 19cm. Light was supposed to emit from all the 360° angles around the lamp, so to trace the emitted light from the simulator in a simple way, a small angles of 10° each were selected around the lamp diameter. Considering rays will flux from this part to the surroundings objects. Light will strike the reflector which is in a trove shape having a base of 8cm and an aperture of 14cm. Taking into the consideration the basics of the light reflection laws, the simulator rays tracing is given in the following figure.

From the theoretical solar simulator ray-tracing that is presented in figure (3), it is noticed that rays emit from the four lamps array of 8k.Watt (2 x1 k.Watt each) form the trove aperture shape, and it covers uncomplete pyramid shape for the room space in the front of the lamps. The uncomplete pyramid shape has two bases, the small one is the lamps tray and the wide one is away from the lamps and its dimensions increase with the distance. The largest base (H) height, is given in figure (4). with a correlation coefficient of 0.99 in cm, determined from the following formula:

$$H = 3.14S + 7.51 \qquad (3)$$

Where, (H) is the height of the rays in cm, and (S) is the distance between the lamps and the object to be investigated in cm as it is given in figure (3). This relationship assists the experiments arrangement under the solar simulator.

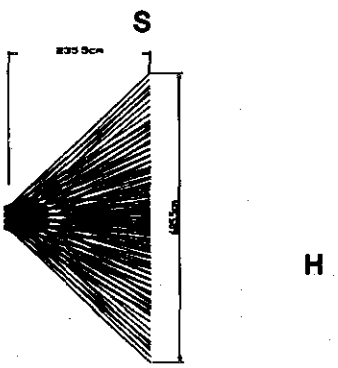

Figure (3): A side view illustration for the ray tracing from the simulator

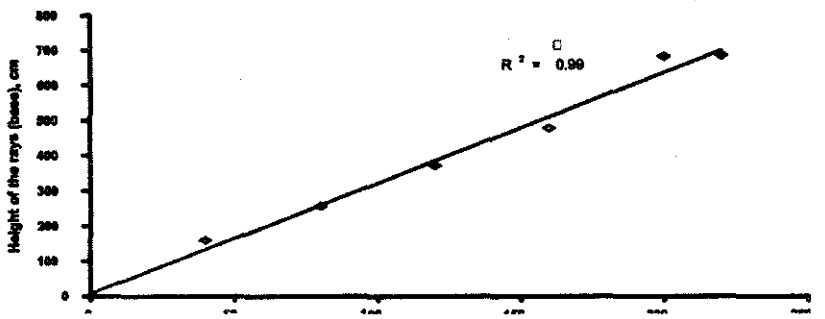

Figure (4): The relationship between the distance (S) from the lamp source and the height of the emitted rays (H) in cm.

Wind tunnel:

Due to the relationship between the wind speed and the convective heat loss coefficient, wind tunnel was required to investigate the effect of the crosswind on the obtained heat exchange effectiveness of the investigated plates. A small open circuit wind tunnel was constructed from centrifugal fan and a 200mm by 200mm-square shape cross section tunnel with a length of 500mm and 1mm aluminum wall with a screen mesh that was mounted on the outlet square shape orifice. The fan has a characteristic of 150mm diameter air suction fan model WME-150, 220-240 Volt (50 Hertz), 0.13 Ampere, Chinese made. 36 points were selected to average the fan output air velocity using the tunnel that is shown in figure (2) while the fan R.P.M. was measured by tachometer. An electric switch was used to vary the fan velocity as a result of the input current to obtain different flow rates of air. Table (2) gives the wind tunnel fan calibration results, while table (3) gives the average monthly wind speed (ms^{-1}) for Ismailia from **Smith (1993)**.

Methods and Measurements:

Radiation:

Mono-crystalline solar cell with dimensions of 75mm x 75mm, with a differential potential of 0.5volt and a current of 800milli ampere was used to measure the fluxed radiation from the lamps under study. A digital US Blaster, Professional Series Multi-meter was used to determine the cell circuit current according to (**Mujahid and Alamoud, 1988**). Calibration series was carried out on the solar cell against an Aply Pyranometer, US made (before, during and after using the cell). The resulted formula from the calibration that was used to determine the incident solar radiation is given in the following form (**Hassanain, 2003**):

$$\text{Global solar radiation in } Wm^{-2} = 1683.5\,(\text{Short circuit current in ampere}) + 32.5 \qquad (4)$$

Table (2): The wind tunnel fan speed

	Velocity I	Velocity II	Velocity III	Velocity IV
Fan R.PM.	1200	1800	2200	2500
Average air velocity, ms^{-1}	0.86	1.29	1.35	1.51
Average discharge, m^3s^{-1}	0.035	0.052	0.054	0.06

Table (3): Average monthly wind speed (ms^{-1}) for Ismailia **(Smith, 1993)**

Jan.	Feb.	Mar.	Apr.	May	Jun.	Jul.	Aug.	Sep.	Oct.	Nov.	Dec.
1.6	1.81	2.09	1.9	1.7	1.4	1.7	1.6	1.4	1.4	1.2	1.4

Investigations were carried out under Tungsten-Halogen-Lamp (THL) with four different artificial illumination sources of 2kW, 4kW, 6kW and 8kW to find out the best choice to simulate the solar energy intensity flux in Ismailia region.

A movable horizontal arm-scale was fitted on a vertical stand of 2.5m height with a 2.4m length was used to fix the cell which was connected to an AVO-meter. The stand with the horizontal arm-scale was fitted on a movable base of 50cm height. The simulator room ground was divided into squares of 10 cm x 10 cm each to facilitate the radiation intensity measurements. Measurements were taken every 10cm on the three main axes (x, y, and z) for the simulator room space.

Radiation measurements were taken for the four sources for each 10cm x 10cm x 10cm of the three main axis x, y, and z of the simulator room space. This was achieved by dividing the solar simulator room ground into 10cm each and using the movable scale to get the x, y and z for each ten centimeter for the room space. The radiation distribution intensity in the test lounge and how it looks like was considered. Also the time lack to reach stable lamp output radiation intensity was considered using different intervals to switch the following lamps row.

Temperatures:

Inlet, outlet, ambient air and surface temperatures were measured with accuracy of 0.1°C using Ama-Digit Ad 15th, electronic thermometer, which had been calibrated before against previously calibrated mercury, -10:100°C-scale thermometer. The standard deviation (SD) between the thermometers reading was ±0.25.

Wind speed and air velocity measurements:

Wind speed and suction air velocity were measured using a TESTO 405-V1 Hot Wire Anemometer meanwhile wind direction was controlled using a protractor to fit the wind tunnel angle with the investigated unglazed transpired surfaces.

The heat exchange effectiveness was determined each two minutes within one hour under exposing the unglazed transpired solar air plates to the solar simulator and half an hour after switching the light off, to imitate the sunny and the cloudy conditions. The suction air was performed within the investigation, while, wind and no wind was performed depended upon the investigation type. Wind speeds (in ms^{-1}) also the wind blowing angle (in degrees, °), were investigated against no wind condition for the different investigated metals which have good conductivity, and the different thickness. The convective heat exchange effectiveness for low suction air flow of $1.3ms^{-1}$, $0.91ms^{-1}$, $0.67ms^{-1}$ and $0.58ms^{-1}$ through thin isothermal perforated plates with and without a cross wind on the up stream face. Different wind speeds, which may be blown in different angles with the investigated plate, were performed.

Wind speeds of $1.51ms^{-1}$, $1.35ms^{-1}$, $1.29ms^{-1}$ and $0.86ms^{-1}$ were performed to find out the prevailing wind speed effect with blowing angles of 0°, 15°, 30°, 45° and 60° compared with no wind conditions.

RESULTS AND DISCUSSIONS

Radiation distribution inside the solar simulator room:

The incident radiation from each lamps-row (2kWatt) at a height of 138cm from the ground datum and along horizontal distance from 0 to 220cm from the lamps aperture is illustrated in figure (5). It was found that the radiation increases inversely with the distance between the lamps and the object being investigated under the solar simulator for different types of the illumination power sources. This is obvious when the radiation intensity was measured for each 10cm apart for the four different types of the illumination power sources as shown in figures (6) and (7).

The radiation distribution inside the simulator room when using the movable stand with the scale arm was carried out for every 10 x 10 x 10cm (which represents x, y and z axis) for the space of the simulator room. The obtained results are shown in figures (6) and (7) for the different distances from the simulator lamps tray aperture of 45cm, 90cm, 135cm, 180cm, and 220cm for left and right distances up to 140cm (each 10 cm apart) from the center of the lamps as it is shown in figure(6).

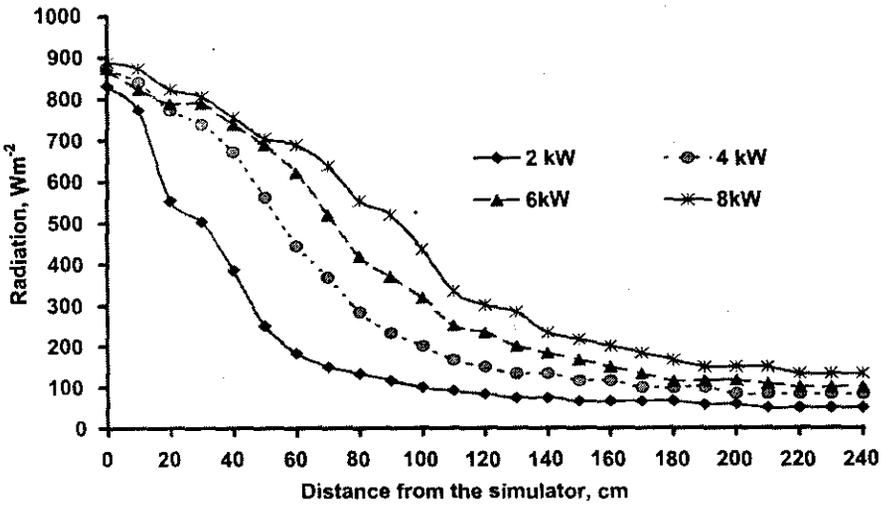

Figure (5): Amount of radiation resulted from each row of the solar simulator (2kW), measured at height of 135cm from the ground datum within distances from 0 to 220cm from the lamp array

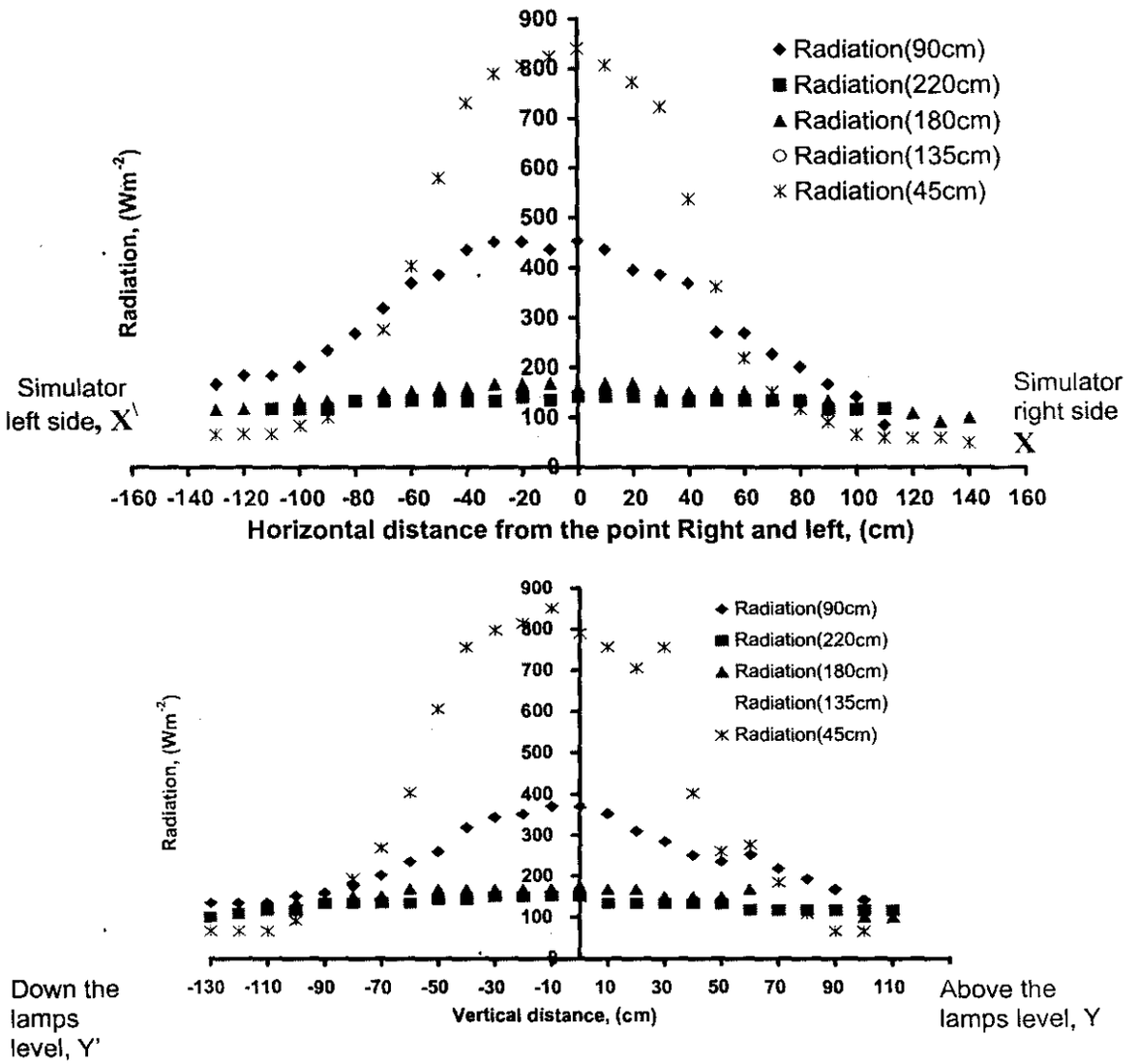

Figure (7): Amount of the measured radiation above and down the lamps level for different distances inside the simulator room, (for lamps of 8kW),

Table (4): Average monthly solar radiation for Ismailia **(Mostafa, 1993)**

Jan.	Feb.	Mar.	Apr.	May	Jun.	Jul.	Aug.	Sep.	Oct.	Nov.	Dec.
452	580	582	643	635	659	632	620	597	525	478	424

Also the radiation flux on the highs are represented in figure (7) for 130cm down the lamp tray central line and 110cm upper the center for the same distances as given in figure (7). From the two figures it is clear that the emitted rays from the used THL gather in the center of the front the aperture as illustrated theoretically in the ray-tracing figure (3). It is noticed that the amount of measured radiation in Wm^{-2} is near to that real solar radiation flux incident on Ismailia region, which is given in the following table.

Also the radiation flux on the highs are represented in figure (7) for 130cm down the lamp tray central line and 110cm upper the center for the same distances as given in figure (7). From the two figures it is clear that the emitted rays from the used THL gather in the center of the front the aperture as illustrated theoretically in the ray-tracing figure (3). This means that experiments can be carried out under the solar simulator to simulate any month all year around with adjusting the distance between the techniques being investigated and the simulator.

Effect of the blowing wind angle and its velocity on the heat exchange effectiveness:

For two minutes interval, the heat exchange effectiveness was determined within one-hour investigations on the effect of the wind speed and its blowing angle. Angles of the blowing wind with the investigated plates of 0°, 15°, 30°, 45° and 60° were compared against no wind conditions. These wind angles, which were the available, as 75° and 90° was not available to be investigated because of the wind tunnel was restricting the incident radiation on the investigated unglazed transpired plates. Figure (8) shows the effect of the angle of the blowing wind on the heat exchange effectiveness for two minutes interval within one hour investigating period, for a galvanized steel of 0.5mm thickness, for an average insolation of 538 Wm^{-2} and wind speed was of $1.5m^{-1}$ also no wind conditions under suction air of $1.3ms^{-1}$. Average of the heat exchange effectiveness ($h\varepsilon_x$) and air temperature increase above ambient ($T_o - T_a$) for the different wind velocities and wind blowing angles, are given in the following table for an 0.5mm thick galvanized steel plates of 2mm (hole diameter) was perforated at square shape of 40mm apart under insolation of $515Wm^{-2}$.

It was found that, heat exchange effectiveness for the same wind-blowing angle increased with the increase of wind speed. Apart of the wind speed of $1.51ms^{-1}$, no trend was noticed for the effect of the blowing wind angle with the surface as it is given in table (5) and shown in figure (8). As the heat exchange effectiveness is affected by the angle of blowing wind only for wind speed of $1.5ms^{-1}$ among the four wind speeds, this wind speed is close to the yearly average wind speed which is ($1.6ms^{-1}$) blowing at Ismailia, the investigation site **(Smith, 1993)**. For the same blowing angle, a direct relationship was found between the blowing wind speed (ms^{-1}) and the value of the heat exchange effectiveness. This emphasis the relationship between the convective heat transfer coefficient and the wind speed of **Watmuff et al., (1977)**.

The suitable suction velocity:

Table (6) represents the effect of the suction air velocity on the heat exchange effectiveness and the temperature-increase above ambient for 5mm thick galvanized steel, under no wind conditions. The plates were perforated by 2mm hole diameters and 40mm square shape spacing. It was found that, there was an inverse relationship between the suction air velocity and the air temperature increase above ambient ($T_o - T_a$). The average heat exchange effectiveness is shown in the following figure with R^2 of 0.94 and the obtained formula that relates the suction air and heat exchange effectiveness as follows:

$$h\varepsilon_x = -0.04v + 0.24 \qquad (5)$$

Nusselt Number was determined for the no wind speed velocity due to the best fit correlation for the normal flow that was obtained by Kutscher(1994) which is given as:

$$Nu_D = 2.75\left(\frac{P}{D}\right)^{-1.2} Re_D^{0.43} \qquad (6)$$

Meanwhile "Nu_D" was calculated according to cross wind as (Kutscher (1994) as:

$$Nu_D = 2.75\left[\left(\frac{P}{D}\right)^{-1.2} Re_D^{0.43} + 0.011\delta\, Re_D\left(\frac{W_s}{v}\right)^{0.48}\right] \qquad (7)$$

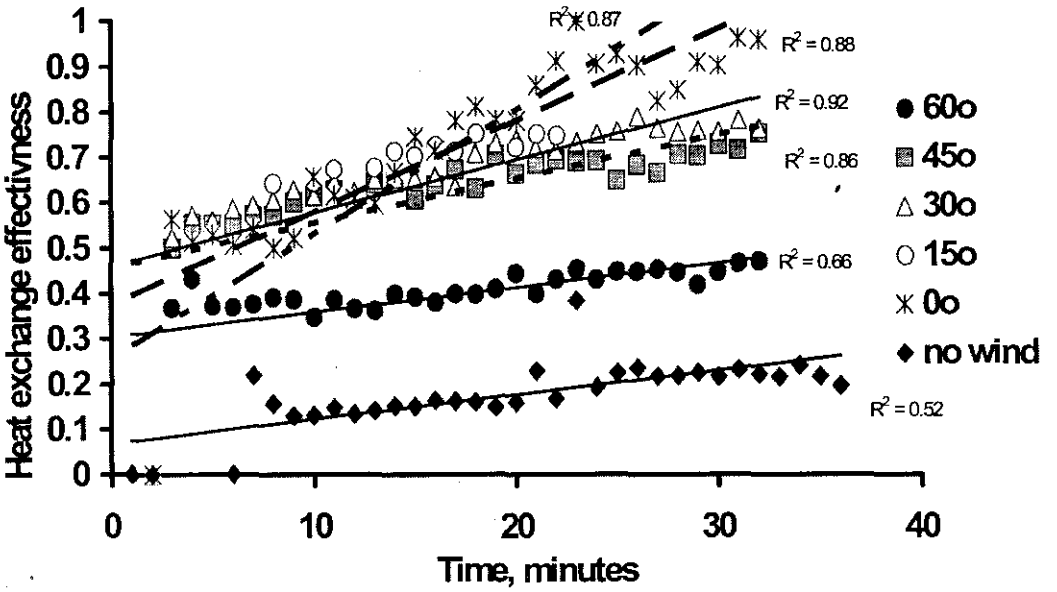

Figure (8): Heat exchange effectiveness affected by the blowing wind angle for 5mm thick galvanized steel with perforation of 2mm hole diameter and 40mm apart square shape at insulation of 538Wm^{-2} with effect of wind speed of 1.5ms^{-1} with the surface under suction of 1.3ms^{-1}.

Table (5): Heat exchange effectiveness for 5mm thick galvanized steel with perforation of 2mm hole diameter at 40mm spacing square shape at average suction air velocity of 1.3ms^{-1} and insolation of 515.42Wm^{-2}.

Wind speed, ms^{-1}		Wind angle with the surface					Without wind
		0°	15°	30°	45°	60°	
1.51	Heat exchange effectvenes	0.698	0.540	0.499	0.465	0.409	$h\varepsilon_x$of 0.192 and (T_o-T_a) of 5.95 °C
	T_o-T_a, °C	4.31	5.12	5.10	4.85	3.90	
1.35	Heat exchange effectvenes	0.341	0.374	0.354	0.337	0.349	
	T_o-T_a, °C	4.09	3.86	4.31	3.58	3.76	
1.29	Heat exchange effectvenes	0.276	0.361	0.328	0.325	0.3394	
	T_o-T_a, °C	3.84	3.63	4.13	3.88	3.98	
0.86	Heat exchange . effectvenes	0.279	0.311	0.318	0.292	0.313	
	T_o-T_a, °C	4.23	4.45	4.69	4.01	3.93	

Table (6): effect of the suction air on the heat exchange effectiveness and temperature increase above ambient (T_o-T_a), for 5mm thick galvanized steel and holes diameters of 2mm with 40 x 40mm square shape spacing under conditions of no wind and incident radiation of 458.6 W/m^2 and suction air velocity of 0.91ms^{-1}.

Suction velocity, ms^{-1}	Heat exchange	S. D.	Average T_o-T_a, °C	S. D
0.58	0.220	0.005	6.96	0.20
0.67	0.211	0.003	6.61	0.13
0.91	0.235	0.003	6.79	0.14
1.30	0.192	0.009	5.07	0.35

Nusselt number is given in figure (10) against the blowing wind speed in ms^{-1} while it is given in figure (11) against the suction air velocity (ms^{-1}). From these figures, Nusselt number increases with the blowing wind speed (in ms^{-1}) and decreases with the suction air velocity.

Plate thickness:

Figure (12) represents the heat exchange effectiveness for different galvanized steel thickness of 0.5, 0.9, 1.2, and 1.4mm as an instance for the other investigated materials, involved in this study. Among these thickness, it was found that the highest obtained $h\varepsilon_r$ value was from the galvanized steel 0.9mm thick.

Unglazed transpired heater materials:

The investigated, good thermal-conductor-metals (isothermal materials) that have the given properties in table (1) were compared to find out the suitable material for the unglazed transpired solar air heaters. A comparison between the galvanized steel plates with the same thickness of steel for all the investigated thickness found that the steel plates gave higher heat exchange effectiveness over the galvanized steel by 13%. Also the aluminum plates gave higher heat exchange effectiveness compared with the same thickness of the galvanized steel. For instance, the heat exchange effectiveness for plates of thickness 1.4mm punctured with 2mm hole diameters at the no wind conditions was investigated under average incident radiation of 398.1Wm^{-2}, were 0.314 and 0.279 with standard deviations of 0.484 and 0.0195 for the Aluminum and Galvanized steel respectively. The aluminum plates showed an increase in heat exchange effectiveness above that for the galvanized steel with the same thickness of 14.2%. It is shown in the following figures a comparison between steel against galvanized steel plates of thickness 1.2mm for instance (figure, 13) while, figure (14) shows a comparison between aluminum against galvanized steel plates of thickness 1.4mm.

From the obtained data, It was found that, the three investigated materials that may be used to design and build the unglazed transpired solar air heaters can be arranged in descended order as a the obtained results of the heat exchange effectiveness values as: aluminum, steel, galvanized steel plates. But, the cost of the material to be used must be considered.

The suitable perforation diameter:

Table (7) represents the changes of the heat exchange effectiveness as a result of changing the hole diameter for the same investigation conditions of suction air velocity of 0.58ms^{-1}, the same surface material and thickness (Galvanized steel of 0.5mm thick), perforation spacing of 40mm square shape and average incident radiation of 398.1Wm^{-2}. Meanwhile, figure (15) represents a linear fitting for the effect of the hole diameters on the temperature increased above ambient ($T_o - T_a$) under the previously mensioned circumstances.

Suitable perforation spacing:

A range of the ratio P/D (peak between the perforating centers /hole diameter) of were investigated and the results were addressed. The distribution was followed squares and diamonds shapes of 80x80mm, 40x40mm, 20x20mm and 10x10mm square shapes and 57x57mm, 29x29mm and 14x14mm diamond shapes. The heat exchange effectiveness resulted from the investigation are presented in the following table and figure, these investigation were carried out on the best perforating hole diameters resulted from the previous investigations of 3mm hole diameters, suitable suction air velocity of 0.91ms^{-1} for 1.2mm steel thick under average insolation of 474.7Wm^{-2}. From table (8) the heat exchange effectiveness is inversely proportional with the P/D for all the squares and diamond which involved with all dimensions. But when (T_o-T_a) were addressed in the comparison the 29x29 mm diamond shape gave the highest value of 5.10°C temperature increase above ambient. As the aim for the unglazed transpired solar air heaters is to obtain higher temperature above the conventional solar air heaters, this design will be considered as the best design option. Taking into the consideration the common designed of the hole diameter is 2mm hole diameter distributed on square shape of 40x 40mm apart as: **Brunger, (1994); Dymond, and Kutscher (1995); Halawa et al., (1997); Hassanain (2000) and Hollick, (1990)**.

From table (8), it is noticed that heat exchange effect has a direct relationship with the number of holes on the same area; but the temperature increase above ambient was increased till cretin dimensions and design. This design was a diamond shape with 29 x29mm so it will be the selected design option compared with other designs, which are given in table (8).

CONCLUSIONS

The study conducted to the following conclusions:

Tungsten-Halogen Lamps (THL) can be used to simulate the sunrays at the experiments site in a repeatable condition for the different applications. It can simulate the incident radiation in Ismailia for the different months, Also, it is cheaper comparing with the other artificial illumination resources.

A direct proportionality was found between the lamps in use and the intensity of the radiation received at different locations inside the solar simulator.

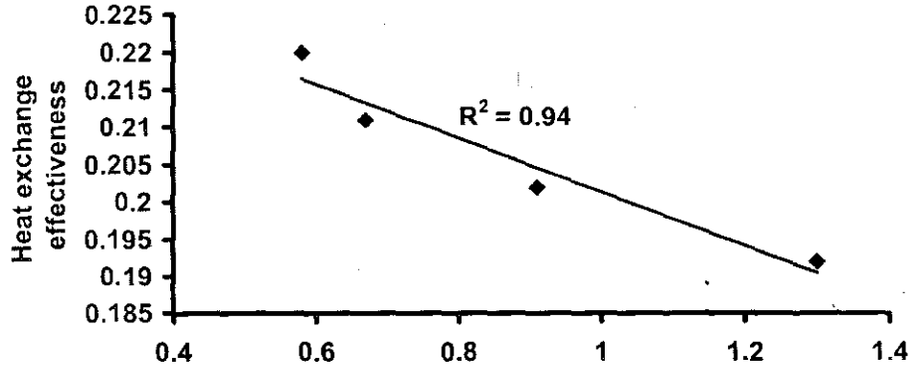

Figure (9): Heat exchange effectiveness as affected by the suction velocity of 0.91ms^{-1}, with no wind speed of 0ms^{-1} and incident radiation of426.4 Wm^{-2} for 0.5mm thick galvanized steel perforated by 2mm hole diameter with square shape of 40 x 40mm spacing.

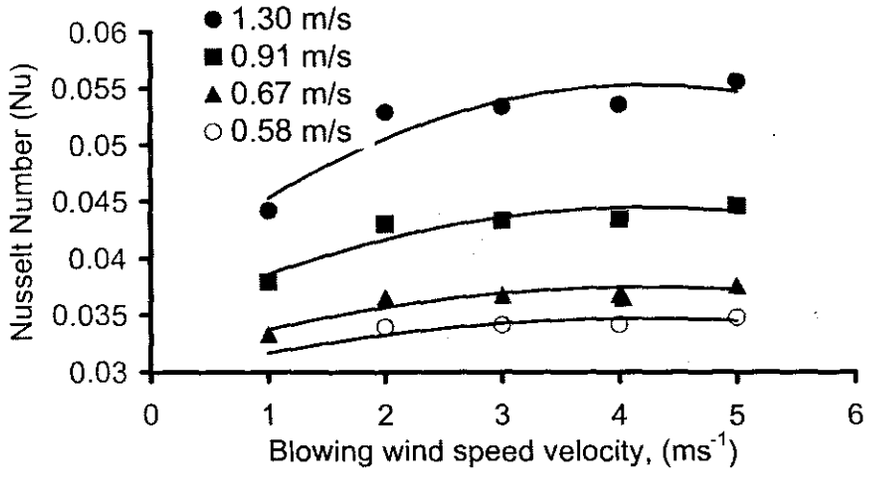

Figure (10): Nusselt number against the different blowing wind speed (in ms^{-1}) as affected by the suction air velocities, ms^{-1}.

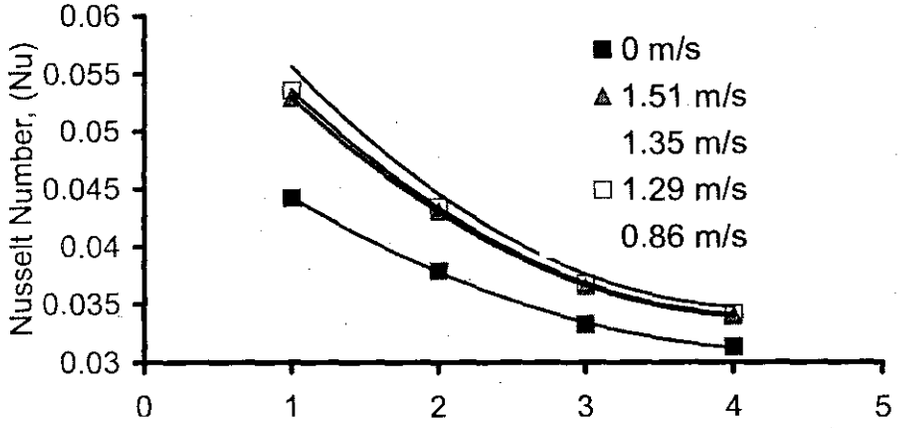

Figure (11): Nusselt number against the different suction air velocities (ms^{-1}) under no wind conditions.

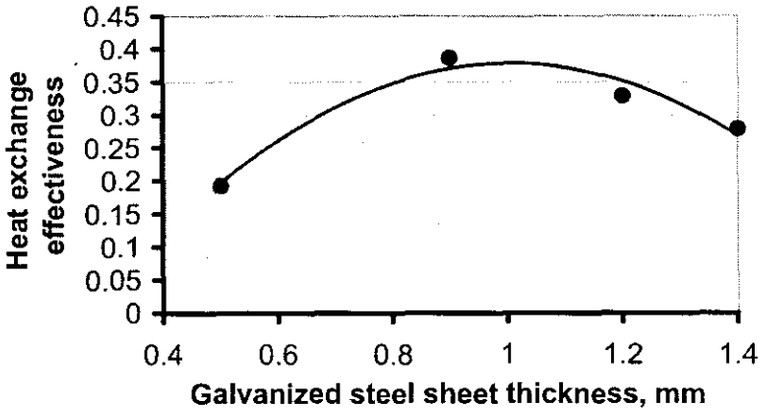

Figure (12): Heat exchange effectiveness as affected by the galvanized steel thickness

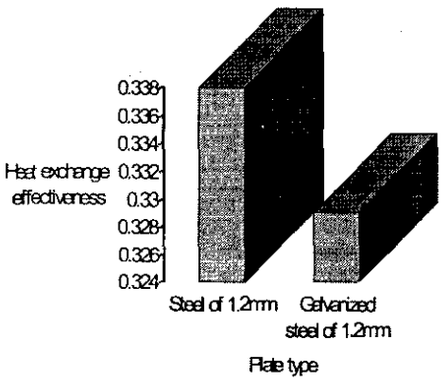

Figure (13): A comparison between the heat exchange effectiveness for steel and galvanized steel under the same investigation conditions.

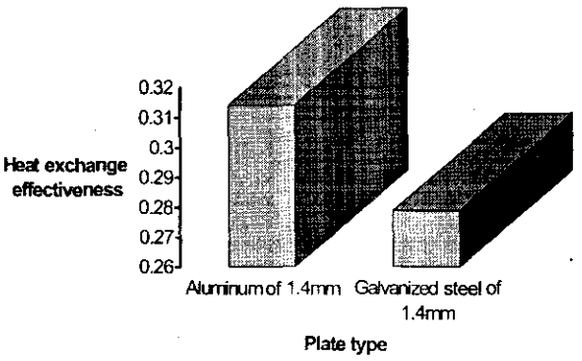

Figure (14): A comparison between the heat exchange effectiveness for steel and aluminum plates under the same investigation conditions

Table (7): Heat exchange effectiveness for different hole diameters for 0.5mm thick galvanized steel with 40x 40mm distance apart, suction air of 0.58ms-1 and no wind speed and incident radiation of 398.1Wm^{-2}.

Hole diameter, (mm)	(2)	(3)	(4)	(5)	(6)
Prosity (δ), Hole area / un-perforated area, (%)	0.19	0.44	0.79	1.23	1.77
P/D	20.0	[illegible]	10.0	8.0	6.7
Average Heat exchange effectiveness	0.220	0.462	0.313	0.354	0.382
S. D	0.01	0.04	0.02	0.03	0.03
$T_o - T_a$, (°C)	7.0	8.5	8.1	9.2	9.4
S. D.	0.20	1.34	1.25	1.06	0.79

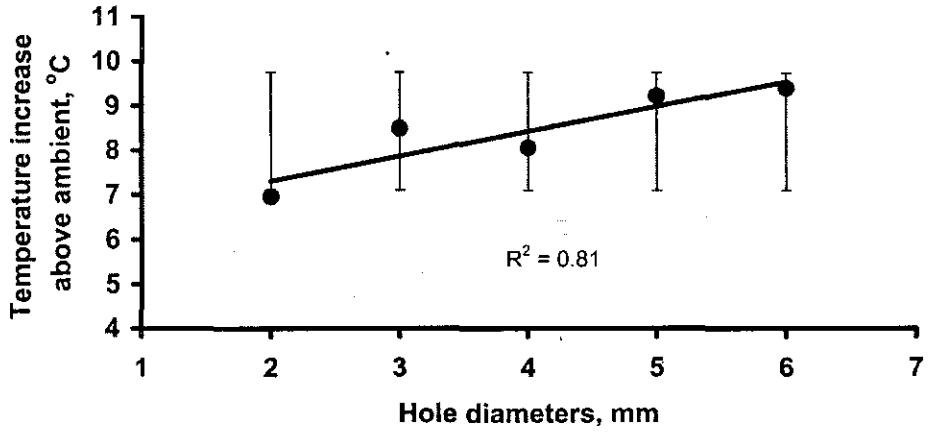

Figure (15): Effect of the hole diameter on the temperature increase above ambient

Table (8): Suitable distribution for the perforating spacing. Investigations were carried out using the best hole diameters of 3mm, suction air velocity of 0.91ms^{-1}, no wind speed and 1.2mm steel thick. (Average insolation of474.7Wm^{-2}).

Shape and dimensions	Squares of 80 x 80mm	Diamond of 57x57mm	Squares of 40 x 40mm	Diamond of 29x29mm	Squares of 20 x 20mm	Diamond of 14x14mm	Squares of 10 x 10mm
P/D	26.7	19	13.3	9.7	6.7	4.7	3.3
Average Heat exchange effectiveness	0.200	0.204	0.236	0.288	0.304	0.358	0.425
S. D	0.093	0.205	0.239	0.006	0.01	0.007	0.00003
$T_o - T_a$, °C	3.70	4.40	4.80	5.10	4.80	4.70	3.50
S. D.	1.213	1.057	0.859	0.157	0.136	0.124	0.002

- Meanwhile, a reverse proportional relationship was found between the incident measured radiation and the distances from the lamps array.
- The theoretical ray tracing for the 8kW solar simulator has conducted to a relationship between the distance from the lamps in use and rays largest base height. The rays-base height in cm was found to follow the following:

Where H is the rays- height in cm, and S is the distance from the lamps in cm.

- A direct relationship was found between the blowing wind angle and the value of the heat exchange effectiveness only for the wind speed of 1.5ms^{-1} which is near the yearly average of wind speed on the experiments location. Meanwhile, a direct relationship prevailed between the wind speed in ms^{-1} for the same blowing angle and the heat exchange effectiveness.
- Nusselt number was found to increase with the blowing wind speed, while it decreases with the suction air velocity.
- The suitable thickness of the unglazed transpired solar air heaters was found dependent upon type of metal in use to manufacture the heater. It was found that the highest obtained $h\varepsilon_x$ value was from the galvanized steel, steel and aluminum plates 0.9mm thick.
- The three investigated materials that may be used to design and build the unglazed transpired solar air hears can be arranged in descended order as: aluminum, steel, galvanized steel plates with taking cost in the considerations.
- The highest obtained heat exchange effectiveness w $H = 3.14S + 7.51$, 3mm for all the investig different conditions.
- Diamond shape distribution for holes with dimensions of 29x29mm spacing gave higher heat exchange effectiveness above the common used shape (square shape).
- Suction air velocity with 0.91ms^{-1} was the best air velocity to give high $h\varepsilon_x$.

Further research and recommendations:

Effect of dust and sandy storms which is blowing in the region of the Suez-Canal and Sinai region should be considered in the further research on the unglazed transpired solar air heaters.

NOMENCLATURES

Nu_D	Nusselt Number based on holes diameter
P	Hole pitch, i.e., distance between center of hole and center of next closest hole, m
D	Hole diameter, m
Re_D	Reynolds number for air flowing through the holes in the absorber
δ	Plate (surface) prosity (hole area/collector area)
W_s	Wind speed, ms^{-1}
v	Average suction air velocity on the plate aparture, ms^{-1}
$h\varepsilon_x$	Heat exchange effectiveness
S	Distance from the lamps
$S.D.$	Standard deviation
H	Height of the light inside the simulator room
T_a	Ambient air temperature, °C
T_s	Surface temperature, °C
T_o	Outlet air temperature, °C

REFERENCES

Ahmed, S. N. (1991) Theoretical and experimental studies on the evaluation of pump for photovoltaic

powered water pumping and its application in Pakistan. Ph.D Th. Department of Engineering, Reeding University, UK.

Brunger, A. P. (1994) Collector efficiency and heat loss of the solar wall at GM Canada, Oshawa:

Interim report prepared for the IEA Solar Heating and Cooling Task 14 Meeting Sevilla, Spain.

Duffie, J. A. and Beckman, W. A.(1991) Solar Engineering of Thermal Processes. John Wiley & Sons, New York, USA.

Dymond, C. S. and Kutscher, C. F. (1995) A computer design model for transpired solar collector systems. ASME, Journal of Solar Energy Engineering, 2: 1165-1175.

Gawlik, K. (1998) National Renewable Energy Lab Develops Low-Cost, Solar Collector. Scientific

Computing & Automation, 11: 15-16.

Green, A. A. and Gillett, W. B. (1979) The significance of longwave radiation in flat plate solar collector testing, IEE conference Proceeding, Future Energy Concepts, London, UK.

Halawa, E. E., Brojonegoro; A. and Davies, R. (1997) An overview of the ASEAN-Canada project on solar energy in drying processes. Drying Technology, 15, 5: 1585-1592.

Hassanain, A. A. (2000) Investigation of solar chimney and tubular transpired solar air heaters as improved systems for solar dryer, Dphil (2000), Faculty of Engineering, University of Ulster, UK.

Hassanain, A. A. (2003) Thermal performance for an unglazed transpired solar dryer (in publishing in Misr Journal of Agriculture Engineering).

Hollick, J. C. (1990) Conserval Solar Air Heating System -Design Manual. Conserval Engineering Inc., Canada.

Incropera, F. P and DeWitt, D. P. (1996) Fundamentals of Heat and Mass Transfer. John Wiley and Sons: 886.

International Organization for Standardization, ISO (1992) International Standard-Solar Energy-

Reference Solar spectral irradiance at the ground at different receiving conditions, Part1, Direct normal and hemispherical solar irradiance for air mass 1.5. ISO-9845-1, 1st Edition.

Kamanga, M. H. (1987) Solar air heaters for drying systems. Master of science thesis, Department. of Agricultural Engineering, University of Newcastle Upon Tyne, UK (unpublished).

Kutscher, C. F. and Christensen, C. B. (1992) Unglazed transpired solar collectors. Advances in Solar Energy ASES, (Ed. Karl W Boer),7: 283-307

Mostafa, M. N. (1992) Solar Energy Equipment, (textbook), Faculty of Engineering &Technology, Helwan University, Egypt.

Mujahid, A. M. and Alamoud, A. R. M. (1988) An easily designed and constructed photovoltaic pyrheliometer, Solar & Wind Technology journal, 5, (2), 127-130.

Norton, B. (1992) Solar Energy Thermal Technology. Springer-Verlag, London: 279.

Pekruhn, W. and Germer, R. (1980) Solar Simulator, Technical note. Solar Energy, 25: 381-383.

Phonix® Electric Co., Ltd, Head Office: Himeiji-City, Hyogo, Japan

Smith, M. (1993) CLIMWAT for CROPWAT, FAO methodology for crop irrigation and drainage.

Paper No. 49 FAO of the United Nations, Rome: 113.

University of Ulster Newsletter (1995), Faculty of Engineering, School of The Built Environment, Jordanstown, BT 37OQB, Northern Ireland, UK

Watmuff, J. H., Charters, W. W. S. and Proctor, D. (1977) Solar and Wind induced external coefficient in solar collectors. COMPLES, 2, 26. (C.F.) Duffie, J. A. and Beckman, W. A. (1991) Solar Engineering of Thermal Processes. John Wiley & Sons, N. Y., USA.

Appendices

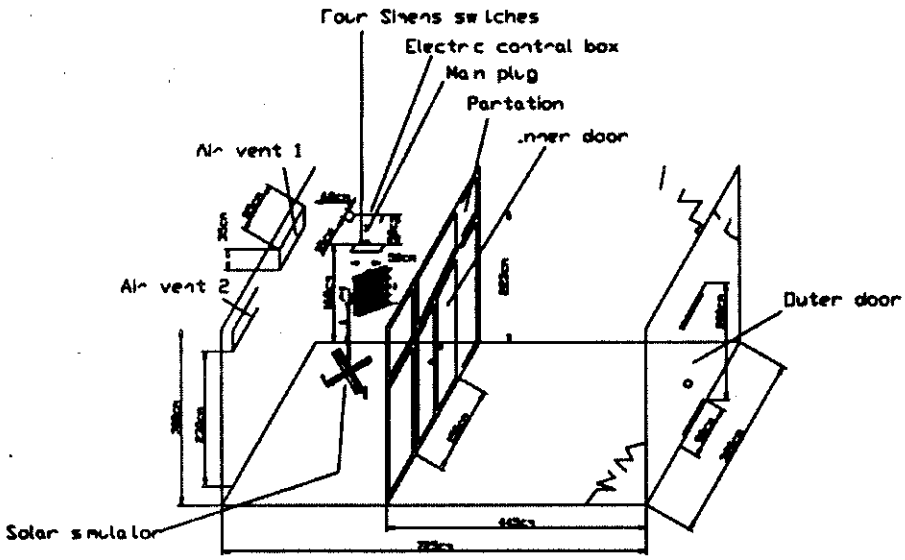

Figure A1: The solar simulator room

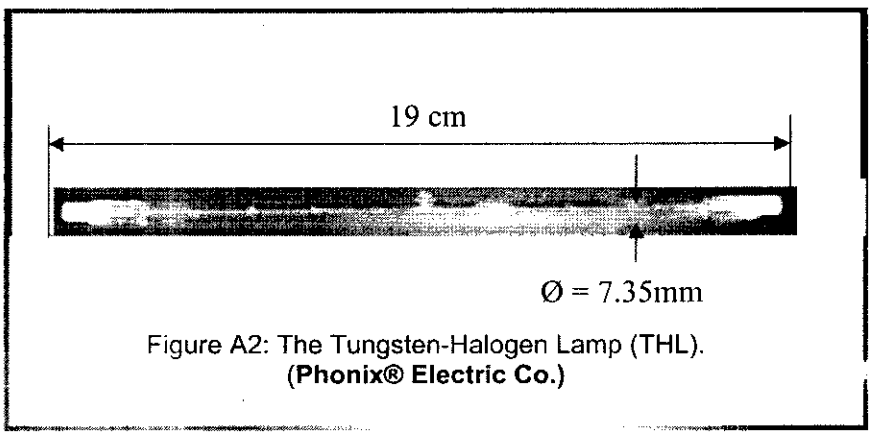

Figure A2: The Tungsten-Halogen Lamp (THL).
(Phonix® Electric Co.)

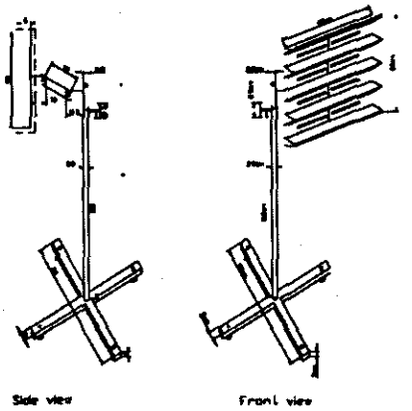

Figure A3: Side and front views for the solar simulator

الملخص العربى

دراسة على الاعتبارات الهندسية لتصميم سخانات الهواء الشمسية المثقبة بدون أغطية شفافة تحت الظروف المصرية

د أحمد على حسانين*

أجريت دراسة لإيجاد أنسب الاعتبارات الهندسية الواجب أخذها عند تصميم سخانات الهواء الشمسية المثقبة، بدون أغطية شفافة بشعبة الميكنة الزراعية – كلية الزراعة جامعة قناة السويس بالإسماعيلية. و قد اختير معامل التأثير الحراري المتبادل على أنه مقياس لمقارنة التصميمات المختبرة حيث انه مؤشر لدرجات حرارة الهواء المكتسبة من السطح تحت الأختبار، و هو عبارة عن نسبة الارتفاع في درجة حرارة الهواء عند درجة حرارة الجو المحيط إلى الارتفاع في درجة حرارة السطح المختبر عن درجة حرارة الجو المحيط. حيث أن أبحاث الطاقة الشمسية تجرى في بيئة متغيرة من كمية الإشعاع الشمسي الساقط، سرعة الرياح، درجة حرارة الجو، فلا تكون هناك فرصة لتكرار تجربة ما لذا فقد تم إنشاء و اختبار مماثل للضوء الشمسي لأجراء التجارب وتكرارها في جو مماثل و محكم . و قد أجريت هذه الدراسة في معمل لمضاهى شمسي نظرا لعدم إمكانية إجراء الدراسة في البيئة الطبيعية كونها متغيرة في كمية الإشعاع الشمسي الساقط و سرعة الرياح و درجة حرارة الجو المحيط و نسبة تركيز الأتربة في الجو المحيط.

و تمت الدراسة بإنشاء مماثل للضوء الشمسي و مماثل لسرعة الرياح و تجاهها على غرفة سحب الهواء و الذي يحوى لوح السخان الشمسي المثقب تحت الاختبار. وقد استخدمت مصابيح من التنجستين-هالوجين قدرة الواحدة منها ١ كيلووات. و قد تم اختبار كمية الأشعة الساقطة من مصابيح ذات قدرة مختلفة للوصول لأنسب قدرة مصابيح تضاهى كمية الأشعة الشمسية الساقطة على منطقة الدراسة وهى الإسماعيلية خط عرض ٥٨و٣٠° (شمالا) و خط طول ٢٣و٣٢° (شرقا). وقد تم اختبار أربعة قدرات من المصابيح و هي ٢ كيلووات و ٤ كيلووات و ٦ كيلووات و ٨ كيلووات و تم دراسة انتشار و توزيع الإشعاع الساقط داخل معمل المضاهى الشمسي أيضا. تم دراسة ثلاثة أنواع من المعادن جيدة التوصيل الحراري، و التي يمكن استخدامها في تصنيع سخانات الهواء الشمسية المثقبة و التي بدون لأغطية شفافة و هي الحديد و الحديد المجلفن و الألومنيوم كلا بسمك ٠,٥، ٠,٩، ١,٢ و ١,٤مم على الترتيب. تم تثقيب المعادن الثلاثة السابقة بثقوب أقطارها ٢، ٣، ٤، ٥، ٦مم على مسافات بينية لتعطى شكلين هما المربع و المعين المتساوي الأضلاع. وقد درس توزيع الثقوب على الأشكال المربعة بأبعاد ٨٠ x ٨٠، ٤٠ x ٤٠، ٢٠ x ٢٠ و ١٠ x ١٠مم وكذلك أشكال المعين المتساوي الأضلاع بأبعاد ٥٧ x ٥٧، ٢٩ x ٢٩، ١٤ x ١٤مم على التوالي و أجريت عليها سرعات سحب الهواء وسرعات الرياح و اتجاهاتها و تأثيرها.

و قد أجريت الاختبارات تحت سرعات شفط مختلفة: ٠,٥٨، ٠,٦٧، ٠,٩١ و ١,٣م/ث على الترتيب و تأثير سرعات رياح مختلفة وهى: ٠,٨٦، ١,٢٩، ١,٣٥ و ١,٥١ م/ث، كل سرعة لها الاتجاهات المختلفة التالية: صفر°، ١٥°، ٣٠°، ٤٥° و ٦٠° وهى الزوايا التي لا تحدث إعاقة لوصول الأشعة للسطح تحت الاختبار مثل الزاويتين ٧٥° و ٩٠°.

و قد توصلت نتائج الدراسة إلى الآتي:

- أن تركيز الأشعة الصادرة من المضاهى الشمسي (باستخدام مصابيح التنجستين-هالوجين قدرة ٨ كيلووات) تضاهى كمية الأشعة الشمسية الساقطة على منطقة الإسماعيلية (خط عرض ٥٨و٣٠ درجة شمالا و خط طول ٢٣و٣٢ درجة شرقا و الذي يتراوح ما بين ٤٢٤ وات/متر٢ و ٦٥٩ وات/متر٢ . و أن كمية الإشعاع الصادرة من المضاهى الشمسي تعتمد على عدد المصابيح المستخدمة و كذا المسافة بين المماثل الشمسي و التقنية الشمسية المراد اختبارها.
- هناك علاقة طردية بين عدد المصابيح المستخدمة و كثافة الأشعة الصادرة منها عند مختلف المسافات داخل غرفة المضاهى الشمسي بينما هناك علاقة عكسية بين المسافة من المصابيح و التقنية المختبرة داخل الغرفة.
- بالدراسة النظرية لتتبع أثر الضوء للمصابيح ذات قدرة ٨ كيلووات و التي تظهر الأشعة الخارجة منها على شكل هرم غير كامل ذي قاعدتين إحداهما مصفوفة مصابيح المماثل الشمسي و هي الصغرى بينما القاعدة الكبرى تبعد عن المصابيح ويمكن الربط بين ارتفاع قاعدتها (H) بالسم كمتغير تابع و المسافة بين المصابيح و التقنية محل الاختبار (S) بالسم كمتغير مستقل من العلاقة التالية:
- وجدت علاقة بين زاوية هبوب الرياح و قيمة معامل التأثير الحراري المتبادل حيث وجدت علاقة طردية مع سرعة الرياح م/ث لنفس زاوية هبوب الرياح
- وجد أن رقم "نسلت" يزداد مع زيادة سرعة هبوب الرياح بينما يتناقص مع زيادة سرعة سحب الهواء.
- أفضل سمك لتصنيع المجمع الشمسي المثقب و الذي بدون أغطية شفافة يعتمد على نوع المادة المصنع منها و الانتشار الحراري خلال هذه المادة. و قد تم الحصول على أعلى قيمة لمعامل التأثير الحراري المتبادل للحديد المجلفن (المجلوق) من سمك ٠,٩مم.
- يمكن ترتيب المواد الثلاث المختبرة و التي يمكن استخدامها في تصميم و بناء السخانات الهواء المثقبة في صورة تنازلية مثل الألومنيوم، الحديد، الحديد المجلفن، مع أخذ في الاعتبار تكاليف الإنشاء.
- افضل شكل وصلت إليه الدراسة هو شكل المعين المتساوي الأضلاع و بطول ضلع قدرة ٢٩مم
- أفضل سرعة سحب للهواء وصلت إليه الدراسة هى ٠,٩١م/ث.

الأبحاث المستقبلية و التوصيات:

يجب أن تتضمن دراسة تأثير العواصف الرملية الشائعة في منطقة الدراسة و المؤثرة على سخانات الهواء الشمسية المثقبة و التي بدون أغطية شفافة في الدراسات المستقبلية.

* مدرس الهندسة الزراعية- كلية الزراعة بالإسماعيلية-جامعة قناة السويس.